



Kinetics and mechanism of imidazole-catalyzed acylation of cellulose in LiCl/*N,N*-dimethylacetamide

Haq Nawaz, Paulo Augusto R. Pires, Omar A. El Seoud*

Institute of Chemistry, University of São Paulo, P.O. Box 26077; 05513-970 São Paulo, S.P., Brazil

ARTICLE INFO

Article history:

Received 23 May 2012

Received in revised form 2 October 2012

Accepted 4 October 2012

Available online 12 October 2012

Keywords:

Kinetics

Imidazole-catalyzed homogeneous

acylation

Cellulose

Anhydrides

ABSTRACT

Cellulose acylation by anhydrides (ethanoic to hexanoic) plus tosyl chloride, TsCl, or imidazole in LiCl/*N,N*-dimethylacetamide solution has been studied. Contrary to a previous claim, TsCl does not catalyze acylation. For the diazole-catalyzed reaction, *N*-acylimidazole is the acylating agent. Third order rate constants (k_3 ; 40–70 °C) have been calculated from conductivity data and split, by using information from model compounds, into contributions from the primary- ($k_{3,\text{Prim}(\text{OH})}$) and secondary- ($k_{3,\text{Sec}(\text{OH})}$) hydroxyl groups of cellulose. Values of $k_{3,\text{Prim}(\text{OH})}/k_{3,\text{Sec}(\text{OH})}$ are >1, and increase linearly as a function of increasing the number of carbon atoms of the acyl group. Rate constants and the degree of biopolymer substitution decrease on going from ethanoic- to butanoic-, then increase for pentanoic- and hexanoic anhydride, due to enthalpy/entropy compensation. Relative to the uncatalyzed reaction, the diazole-mediated one is associated with smaller enthalpy- and larger entropy of activation, due to difference of the acylating agent.

© 2012 Elsevier Ltd. All rights reserved.

1. Introduction

Although the acylation of cellulose in LiCl/*N,N*-dimethylacetamide (DMAC) and in other solvent systems, e.g., tetraalkylammonium fluoride hydrate/DMSO by carboxylic acid anhydrides and acyl chlorides is efficiently catalyzed by tertiary amines, e.g., imidazole, Imz, or 4-(*N,N*-dimethylamino)pyridine there is no information on the kinetics and activation parameters of these reactions. This information is important *per se*, and because it allows calculation of the reaction time under a given set of experimental conditions, an important aspect in green chemistry. Additionally, kinetic data are required in order to compare: (1) The efficiency of different catalysts for the same derivatizing agent/solvent; (2) the reactivity of distinct derivatizing agents in the same solvent; (3) the reactivity of celluloses with different structural characteristics, under fixed reaction conditions.

A principle reason for the lack of kinetic studies is that they are laborious, involving determination of the degree of the biopolymer substitution, DS, as a function of reaction time (*t*), e.g., by saponification and subsequent back titration of the residual base. Consequently, the calculation of the observed rate constants, k_{obs} is based on a limited number of data points, e.g., 3–12 (Kwatra, Caruthers, & Tao, 1992; Tosh & Saikia, 2000; Tosh, Saikia, & Dass, 2000). Recently, we have shown that conductivity

is a convenient experimental technique for investigating the kinetics of the uncatalyzed acylation of microcrystalline cellulose, MCC, in LiCl/DMAC (Nawaz, Casarano, & El Seoud, 2012). By using cyclohexylmethanol (CHM, one primary hydroxyl; Prim(OH)) and *trans*-1,2-cyclohexanediol (CHD, two secondary hydroxyls; Sec(OH)) as models for the C6-OH, and the C2-OH plus C3-OH groups, respectively of the anhydroglucose unit, AGU, of cellulose, we were able to split the overall rate constants into contributions from the distinct hydroxyl groups. The dependence of the rate constants and DS on the number of carbon atoms of the acyl group, *N_c*, has been explained based on the reaction activation parameters (Nawaz et al., 2012).

We have now extended this study to MCC-catalyzed acylation in the same solvent system by carboxylic acid anhydrides; ethanoic-, propanoic-, butanoic-, pentanoic-, and hexanoic anhydride (all *normal-chain* compounds). It has been claimed that this reaction is catalyzed by tosyl chloride, TsCl (Tosh and Saikia, 2000; Tosh et al., 2000). The latter reaction however, was not faster than that its uncatalyzed counterpart! By using ¹H NMR, we have shown that the acetylation reaction is not subject to catalysis due to the (claimed) formation of a reactive intermediate (mixed carboxylic-sulfonic anhydride, *vide infra*) which (presumably) reacts with cellulose (Tosh and Saikia, 2000; Tosh et al., 2000). We have then studied the imidazole (Imz)-catalyzed acylation. Use of ¹H NMR and FTIR has confirmed the intermediate formation of *N*-acylimidazole; a combination of kinetic data and theoretical calculations has shown that this is the actual acylating agent, in agreement with previous opinions (El Seoud,

* Corresponding author. Tel.: +55 11 3091 3874; fax: +55 11 3091 3874.

E-mail address: elseoud@iq.usp.br (O.A. El Seoud).

Menegheli, Pires, & Kiyan, 1994; Hussain, Liebert, & Heinze, 2004).

Rate constants and activation parameters have been calculated from the dependence of solution conductivity (λ) on reaction time (t) at different temperatures (T). By using information from the hydroxyl groups of CHM and CHD, we were able to split the overall third-order rate constants (k_3) into contributions from both types of hydroxyl groups. Values of $k_{3;\text{Prim}(\text{OH})}/k_{3;\text{Sec}(\text{OH})}$ were >1 , and increase linearly as a function of increasing N_c . All parameters of this reaction, rate constants, activation parameters, DS, show a nonlinear dependence on N_c , namely: a change from ethanoic- to butanoic anhydride in one direction, followed an opposite change for pentanoic-, and hexanoic anhydride, vide infra. This is attributed to subtle and compensating changes of the reaction enthalpy, ΔH^\ddagger , and entropy, ΔS^\ddagger , to the free energy of activation, ΔG^\ddagger . Relative to the uncatalyzed reaction, the rate enhancement is due to a decrease in ΔH^\ddagger , with concomitant increase in ΔS^\ddagger .

2. Experimental

2.1. Solvents and reagents

All solvents and reagents were purchased from Alfa Aesar, Merck, or Mensalão Cachoeirense Química and were purified as recommended elsewhere (Armagero & Chai, 2003). TsCl was purified by dissolving 10 g in 25 mL of dry chloroform. The solution was filtered, 125 mL of dry hexane was added, the solution filtered, and the solvent evaporated to give a white solid, m.p. 67–68 °C; literature m.p. 67–69 °C (Hacon et al., 2007). DMAC was purified by distillation from CaH_2 . Its purity was established by measuring its density at 25 °C, 0.9372 (DMA 4500D digital densimeter, Anton Paar, Graz) (Lide, 2004). The pH of 20% solution DMAC in water was equal to that of water. The expanded-scale pH paper employed is able to detect $1.4 \times 10^{-4} \text{ mol L}^{-1}$ of diethylamine. MCC (Avicel PH 101) was obtained from FMC, Philadelphia (degree of polymerization by viscosity, $\text{DPv} = 150$); (ASTM 2001) index of crystallinity, I_c , by X-ray diffraction = 0.82 (Buschle-diller & Zeronian, 1992).

2.2. Preparation of solution of cellulose in LiCl/DMAC

LiCl was dried at 300 °C for 2 h, and then cooled to room temperature under reduced pressure. The electrolyte was quickly weighed (6.0 g; 0.141 mol) in 100 mL volumetric flask; 80 mL of dry DMAC were added, the flask was closed with a drying tube and sonicated (Laborrette 17, Fritsch, Berlin) until a clear solution was obtained, ca. 3.5 h. The solution volume was completed to the mark with fresh solvent.

MCC (2.0 g; 12.3 mmol) and LiCl (6.0 g) were weighed into a 250 mL three-neck round-bottom flask. The latter was equipped with a stopcock, 100 mL graduated addition funnel (no equilibration side arm) and a magnetic stirring bar. The flask was immersed into an oil bath, and then connected to a vacuum pump. The pressure was reduced to 2 mmHg, the system was heated to 110 °C in ca. 35 min, and then kept under these conditions for (additional) 30 min. The vacuum pump was turned off, the stopcock closed, the heating bath removed, and 60 mL of pure DMAC were added dropwise. The system was then brought to atmospheric pressure with dry, oxygen-free nitrogen. The addition funnel was substituted by a condenser with a drying tube, and the flask was quickly equipped with an efficient mechanical stirrer. The temperature was raised to 150 °C in ca. 35 min, and the cellulose slurry was vigorously stirred for 90 min (IKA Labortechnik, model RW 20, 500 rpm) at this (bath) temperature. The latter was decreased to $50 \pm 5^\circ\text{C}$ in 2 h, and the slurry was left under these conditions with magnetic stirring overnight; a clear cellulose solution was obtained. The cellulose

Table 1

Experimental details for the imidazole-catalyzed acylation of hydroxyl-carrying compounds (ROH).^{a,b}

ROH	[ROH]; listed as mol L^{-1} (OH)	Anhydride concentration; mol L^{-1}	Imidazole concentration; mol L^{-1}
CHM	0.0288	0.288	0.576
CHD	0.0576	0.576	1.152
MCC	0.0864	0.864	1.728

^a The experiment was carried out by adding 10 mL of ROH in 6% LiCl/DMAC to 5 mL of a solution of acid anhydride plus imidazole in pure DMAC. The final LiCl concentration was 4%, or 0.943 mol L^{-1} .

^b CHM, CHD, and the AGU of MCC carry one, two, and three (OH) groups per molecule, respectively. Therefore the ROH concentrations are listed as moles of (OH)/liter. As shown in the second and third columns, the molar ratios [reagent]/[OH] are 10 and 20 for acid anhydride, and imidazole, respectively.

solution was transferred to 100 mL volumetric flask, whose volume was completed by adding DMAC that has been employed in washing the walls of the round-bottom flask.

2.3. Kinetics of acylation of the model compounds and cellulose

The progress of the acylation reaction was monitored by following the increase in solution conductivity (λ) as a function of (t), at a constant (T). We have employed Fisher Accumet AR-50 ion meter, equipped with Metrohm 6.0910.120 conductivity electrode, inserted in a home-built double-walled conductivity cell through which water is circulated from a thermostat, as shown in previous work (Nawaz et al., 2012). Data acquisition and the solution temperature were controlled with a PC. Temperature control was achieved by using a glass-covered PT-100 sensor inserted into the reaction solution, and attached to the computer via RS-232 serial port.

The experiments were carried out as follows: 5 mL of pure DMAC containing the appropriate anhydride were introduced into the conductivity cell followed by the addition of required amount of solid Imz. After thermal equilibration, the solution of the compound studied (CHM, CHD, or MCC) in 10 mL of 6% LiCl/DMAC was introduced into the conductivity cell. The increase in (λ) was recorded as a function of (t), until its value was practically constant. Table 1 shows the reagent concentrations employed, where the acronym (ROH) is employed to denote any hydroxyl group-carrying compound (CHM; CHD; MCC).

A home-developed non-linear regression analysis program, based on Marquardt–Levenberg algorithm (Press, Teukolsky, Vetterling, & Flannery, 2007) has been employed for calculating the values of the observed rate constants (k_{obs}). It relies on minimizing the sum of the squares of the residuals. The agreement between calculated and experimental “infinity” conductivity (λ_∞) was routinely checked. The relative standard deviation in k_{obs} was $\leq 0.5\%$, that between k_{obs} of triplicate runs was $< 3\%$. The values of (k_3) were obtained by dividing the corresponding $k_{\text{obs}}/[\text{anhydride}][\text{imidazole}]$. The activation parameters were obtained from the dependence of k_3 on T , by using standard equations (Anslyn & Dougherty, 2006).

2.4. Synthesis and analysis of the acetylation products under the conditions of the kinetic experiment

The kinetic experiments were repeated on a larger scale (three fold), as follows: in order to simplify the separation of the acetates of CHM and CHD we used LiCl suspension in acetonitrile as solvent, instead of DMAC. The solvent, 25 mL was introduced into 100 mL three-necked round bottom flask, equipped with a condenser and a drying tube. The bath temperature was adjusted to 60 °C, and 8 mL (84 mmol) of ethanoic anhydride was added, followed by addition of, 1 g LiCl and 11.76 g (0.172 mol) of Imz;

the mixture was stirred for 5 min. The required amount of ROH; 2.14 mL, 17 mmol CHM, or 1.07 mL, 8.6 mmol of CHD was added, and the reaction mixture was stirred for 15 min at 60 °C. After evaporation of the solvent, the residue was carefully neutralized with a cold aqueous solution of NaHCO₃, and then extracted with 30 mL of CH₂Cl₂. The organic layer was washed with cold dilute HCl (in order to remove Imz), with water, dried with anhydrous MgSO₄, and then the solvent was evaporated. The liquid products cyclohexymethyl acetate (79% yield) or *trans*-1,2-cyclohexane diacetate (75% yield) gave IR- (Bruker Vector-22 FTIR spectrophotometer; neat sample, 32 scans at 0.5 cm⁻¹ digital resolution), and ¹H NMR spectra (Bruker DPX 300 NMR spectrometer; CDCl₃) that agreed with the results reported elsewhere; (AIST, 2001; Das, Reddy, & Tehseen, 2006; Khaja & Xue, 2006; Zeynizadeh & Sadighnia, 2010; Zeynizadeh & Sadighnia, 2011) see Fig. SM-1 (Fig. 1 of Supplementary Material) and Table SM-1 (Table 1 of Supplementary Material) for attribution of the IR and ¹H NMR spectral data of the isolated products.

For MCC, the acylation reaction was carried in LiCl/DMAC solution, at 60 °C, as follows: DMAC, 25 mL, was introduced into 200 mL round-bottom flask, equipped with a condenser and a drying tube. Ethanoic-, butanoic-, or hexanoic anhydride, was introduced (1.3 mmol; 1.3-, 2.26-, and 3.2 mL, respectively), followed by addition of Imz (1.77 g, 2.6 mmol). A solution of MCC in 6% LiCl/DMAC was then added (35 mL containing 0.245 g cellulose, 1.3 mmol/OH); the mixture was stirred (N₂ atmosphere) at 60 °C for 35 min. The resulting cellulose ester was precipitated in ethanol; repeatedly suspended in the same solvent (3 × 200 mL; 60 °C), then filtered, washed with water, and dried for 24 h under reduced pressure, over P₄O₁₀, at 60 °C. DS of the ester was determined by titration (ASTM, 2002) DS = 1.93, 1.52, 2.14, for cellulose ethanoate, butanoate, and hexanoate, respectively.

2.5. Corroboration of the mechanism of catalysis: detection of the reactive intermediates formed

¹H NMR (Varian, Gemini-300) and FTIR have been employed in order to detect the reactive intermediates, formed by the reaction between the anhydride and the catalyst, as follows.

2.5.1. ¹H NMR

Equal volumes of solutions in DMSO-*d*₆ of acetic anhydride (0.05 mol L⁻¹) and (0.05 mol L⁻¹) TsCl were mixed in a glass tube, agitated (vortex) and quickly transferred to the NMR tube (Wilma 535pp). The spectrum of the resulting solution was recorded as a function of time. The same experiment was repeated with Imz, by using CDCl₃ as solvent.

2.5.2. FTIR

Equal volumes of solutions in CD₃CN of acetic anhydride (0.42 mol L⁻¹) and Imz (0.42 mol L⁻¹) were mixed in a glass tube, agitated (vortex) and quickly transferred to the IR cell (CaF₂). The spectrum of the resulting solution was recorded as a function of time.

3. Results and discussion

3.1. Acylation by acid anhydrides in the presence of tosyl chloride or imidazole

Our observation that the acetylation of cellulose in LiCl/DMAC (DP = 900; 0.0864 mol L⁻¹) in the presence of TsCl (0.308 mol L⁻¹) (Tosh & Saikia, 2000; Tosh et al., 2000) is not faster than the uncatalyzed acetylation of MCC (Nawaz et al., 2012) begs for an explanation, even when the difference in DP is taken into account. Note that the difference in *I*_c of the two celluloses has no bearing on

the kinetic results because cellulose is decrystallized on dissolution in LiCl/DMAC (Ramos, Assaf, El Seoud, & Frollini, 2005). The reaction mechanism proposed is shown below (Tosh & Saikia, 2000; Tosh et al., 2000) (Scheme 1).

This catalysis, if it occurs, rests on the formation of the mixed anhydride intermediate (structure depicted inside the frame) that is expected to be more reactive than acid anhydride in the acylation reaction. The formation of this intermediate has not been documented (Tosh & Saikia, 2000; Tosh et al., 2000) therefore, we employed ¹H NMR in an attempt to detect its formation; the results are shown in Fig. 1. Parts (A) and (B) of this figure do not indicate a reaction between the two reagents, i.e., there is no detectable formation of the expected mixed anhydride. Therefore, the acetylation is, in fact, not subject to catalysis by TsCl. Note that acetyl tosylate is a stable compound that can be isolated in pure form (Kenichi, 2003a, 2003b); its formation from Ac₂O plus toluene sulfonic acid has been demonstrated by NMR (Liu, Liu, Lu, & Cai, 2008).

We decided to investigate the use of Imz. As shown in Scheme 2, this catalysis, if it occurs, involves the intermediate formation of *N*-acyldiazole, RCOImz, and its subsequent reaction with cellulose. The end products are cellulose carboxylate; carboxylic acid, and (regenerated) Imz. The latter two products react to form imidazolium carboxylate. Fig. 2 shows the ¹H NMR spectra of the two authentic reactants, acetic anhydride and Imz, as well as their mixture in CDCl₃, after 5 min of mixing. The formation of CH₃COImz and CH₃CO₂H is clearly evidenced by the appearance of new singlets at 2.60 and 2.09 ppm, respectively, and by the changes of the chemical shifts of the heterocyclic ring protons, namely: The hydrogen at positions 4 and 5 of Imz are no more equivalent; the large shift (Ha → H'a).

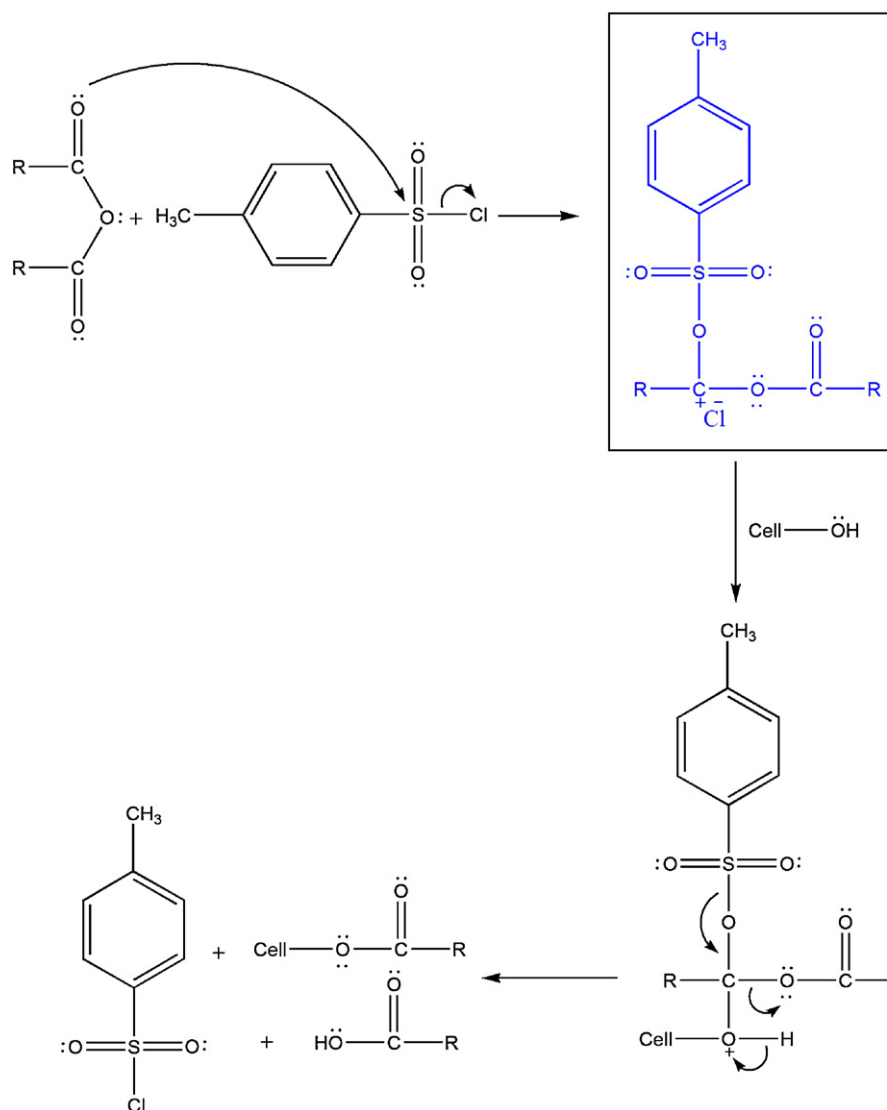
FTIR is a powerful tool in order to show the intermediate formation of RCOImz. As shown in Fig. SM-2, the characteristic anhydride ν_{C=O} "doublet" (due to asymmetric and symmetric stretching vibrations, respectively) at 1821 and 1751 cm⁻¹, are replaced by peaks at 1737 and 1716 cm⁻¹, due to the formation of *N*-acetylImz and acetic acid, respectively. We then proceeded to determine the rate constants and activation parameters of the Imz-catalyzed acylation of cellulose by carboxylic acid anhydrides, from ethanoic- to hexanoic anhydride in LiCl/DMAC.

3.2. Setup of the kinetic experiment and calculation of the individual rate constants

Conductivity is a simple and accurate technique to determine rate constants. Unlike other techniques, e.g., spectroscopy and chromatography, the change in conductivity is only indirectly linked to the reaction. Therefore, we have carried out specific experiments; see Section 2, in order to show that the expected reaction products (esters) of CHM, CHD, and MCC are obtained under the conditions of the kinetic runs. That is, the reaction that is been followed by conductivity is Imz-catalyzed acylation.

The advantage of carrying out kinetic experiments under first-order conditions is that the concentration of the species that is being followed, reactant or product, need not be known. That is, any property that changes proportionally to the progress of the reaction (conductivity, absorption, pH, etc.) can be employed in order to calculate the value of the observed rate constant, *k*_{obs}. The (large) molar ratios anhydride/cellulose and Imz/cellulose shown in Table 1 indicate that the acylation reactions have been carried out under pseudo-first order conditions. This is corroborated by the straight lines shown in Fig. SM-3. Values of the third order rate constants, *k*₃, and the activation parameters are calculated from *k*_{obs} as given in Section 2.

For MCC, *k*₃ refers to the sum of the reactions of one primary hydroxyl-, Prim(OH), plus two secondary hydroxyl groups,



Scheme 1. Suggested mechanism for the catalytic effect of TsCl on the acylation by acid anhydrides. The structure inside the frame is that of the expected intermediate (Tosh and Saikia, 2000; Tosh et al., 2000).

Sec(OH). If the latter hydroxyls are considered equivalent in reactivity (Kwatra et al., 1992; Malm, Tanghe, Laird, & Smith, 1953; Tosh et al., 2000) then:

$$k_3 = k_{3; \text{Prime(OH)}} + 2k_{3; \text{sec(OH)}} \quad (1)$$

Any meaningful discussion of the data requires that these contributions are separated. In order to solve this problem, we have employed CHM as a model for C6-OH, and CHD as a model for C2-OH plus C3-OH of the AGU. With this proviso, the rate constants and the activation parameters of the two types of (OH) groups of MCC have been calculated as a function of Nc. Table 2 shows the overall- and partial k_3 for MCC, along with the corresponding activation parameters. As given in Section 2, all parameters have been calculated for a single hydroxyl group.

The reaction of the model compounds was studied at 50 °C. The values of k_3 for ethanoic-, propanoic-, butanoic-, pentanoic-, and hexanoic anhydride, respectively are: 3.382-; 3.036-; 2.809-; 3.283-; and $3.389 \times 10^{-2} \text{ M}^{-2} \text{ s}^{-1}$ for (CHM); and 1.876-; 1.619-; 1.463-; 1.660; and $1.668 \times 10^{-2} \text{ M}^{-2} \text{ s}^{-1}$ for (CHD). As will be shown below, the ratios ($k_{3; \text{CHM}}/k_{3; \text{CHD}}$) were then corrected.

Considering these data, the following is relevant:

- (i) As shown in Scheme 2, one mol of acetic anhydride reacts with 2 mol of Imz to produce one mol of *N*-acetylImz plus one mol of imidazolium acetate. That *N*-acylimidazole is the actual acylating agent can be shown by several pieces of evidence:
 - Values of k_3 have been calculated for the reaction of CHM (50 °C) with: a mixture of 20 mmol acetic anhydride plus 40 mmol Imz; 20 mmol authentic *N*-acetylImz; 20 mmol authentic *N*-acetylImz in the presence of 20 mmol authentic imidazolium acetate. All rate constants were found to be practically the same, 2.170-; 2.015-; and $1.997 \times 10^{-2} \text{ M}^{-2} \text{ s}^{-1}$, respectively. This result also shows that the imidazolium acetate formed in the reaction has no (acid–base) catalytic effect.
 - Our theoretical calculations have shown that the reaction with RCOImz is more favorable than that with the precursor (RCO)₂O. Thus the partial positive charge on the acyl-carbon of CH₃COImz (0.293 a.u.) is larger than that on the corresponding group of acetic anhydride (0.235 a.u.). Additionally, molecular dynamics simulations were performed on mixtures

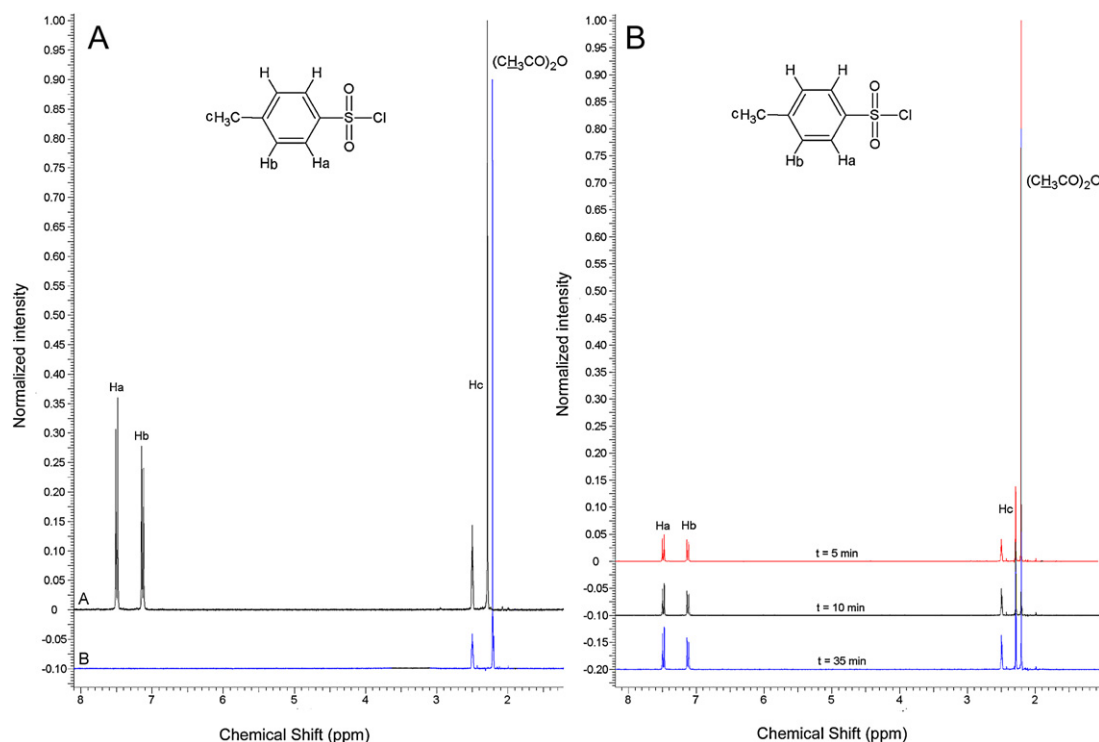
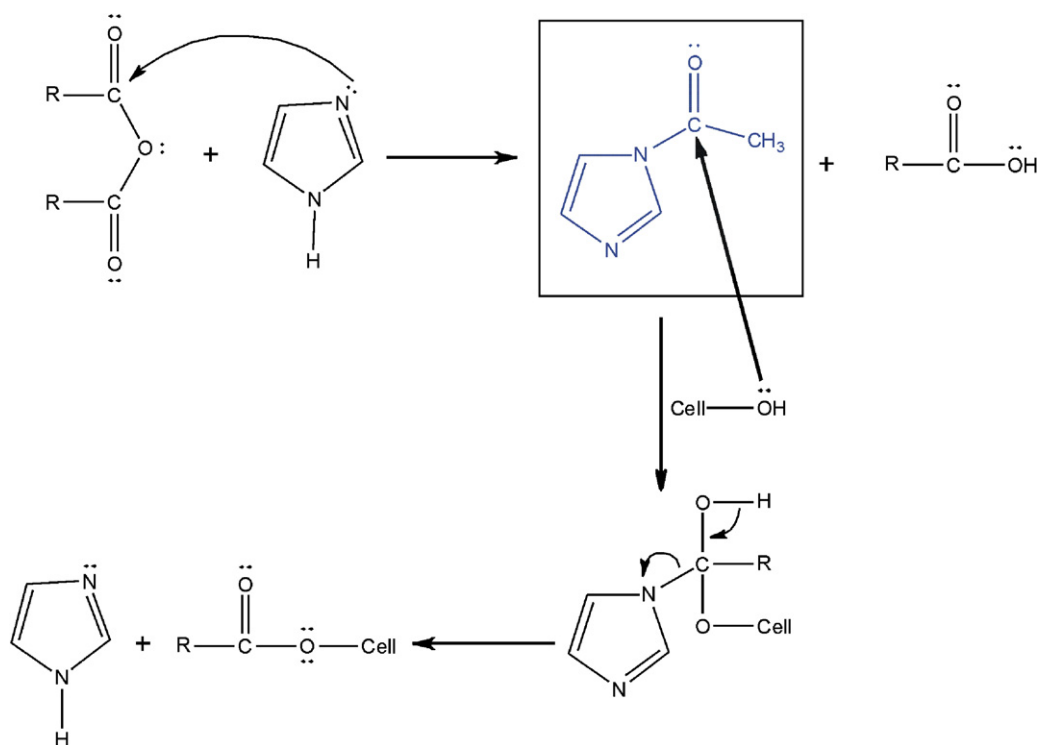


Fig. 1. Part (A) shows superimposed ^1H NMR spectra of authentic samples of acetic anhydride (lower curve) and tosyl chloride (upper curve) in $\text{DMSO}-d_6$ with the discrete hydrogens indicated. Part (B) shows the spectra of a mixture (in the same solvent) of acetic anhydride (0.05 mol L^{-1}) and tosyl chloride (0.05 mol L^{-1}) as a function of time.

containing DMAC and CHM with: Acetic anhydride, or *N*-acetylImz; see Fig. SM-4. The relevant information obtained is that the complex $\text{CHD}/\text{CH}_3\text{COImz}$ remains more time in contact. According to the “spatio-temporal” postulate, molecules will react if they stay at a critical distance for a certain length of

time (Menger, 1985). As Fig. SM-4 shows, these criteria apply to the Imz-catalyzed reaction.

(ii) As given above, the ratios between the reactivities of the model compounds have been employed in order to split the overall k_3 of MCC into contributions from the primary and secondary



Scheme 2. A complete reaction mechanism for the imidazole-catalyzed acylation of cellulose. The reaction sequence involves the intermediate formation of *N*-acylimidazole, followed by its reaction with cellulose to produce cellulose ester, plus imidazolium carboxylate.

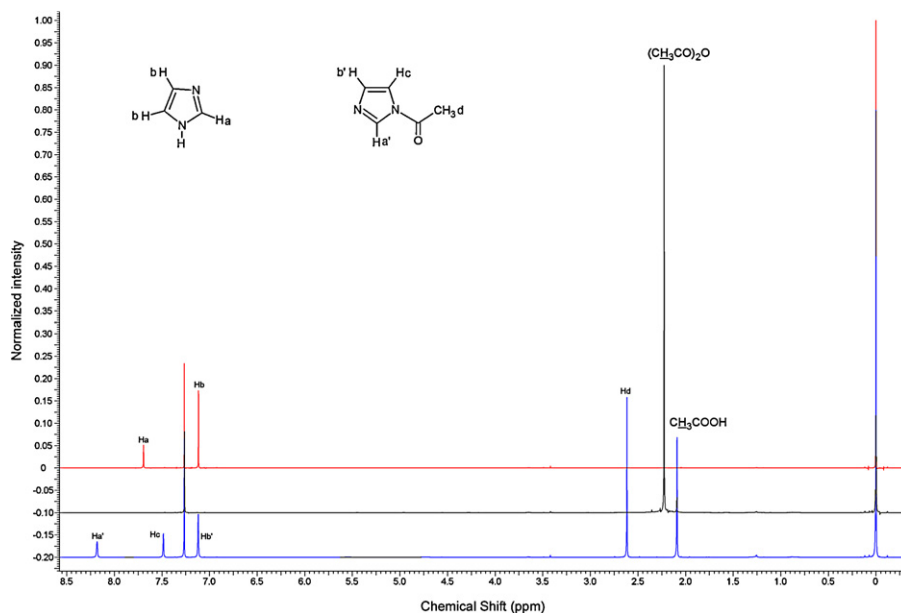


Fig. 2. ^1H NMR spectra in CDCl_3 of authentic samples of imidazole (0.05 mol L^{-1} ; upper plot); acetic anhydride (0.05 mol L^{-1} ; middle plot) and an equimolar mixture of both reactants after 5 min of mixing, lower plot. The discrete hydrogens are labeled.

hydroxyl groups. The reaction of the model compounds with each anhydride in the presence of imidazole shows that the ratio ($k_3; \text{Prim}(\text{OH}); \text{CHM}/k_3; \text{Sec}(\text{OH}); \text{CHD}$) > 1 . To our knowledge, this is the first time that these ratios have been experimentally determined for the catalyzed acylation reaction under homogeneous conditions. The results show that the reactivity ratios increase as a function of increasing N_c , according to the following equation (r = correlation coefficient; SD = standard deviation):

$$\frac{k_3; \text{Prim}(\text{OH}); \text{CHM}}{k_3; \text{Sec}(\text{OH}); \text{CHD}} = 1.697 + 0.056N_c; \quad r = 0.997; \quad \text{SD} = 0.007 \quad (2)$$

Therefore, the outcome of the reaction, in terms of DS at C6- and C2 plus C3 depends on the derivatizing agent; the preference for

the C6 position increases as a function of increasing the molecular volume of the acylating reagent. This agrees with the known fact that it is possible to functionalize cellulose almost exclusively at the C6 position by voluminous reagents, e.g., trityl compounds (Kondo, 1993).

- (iii) The reactivity ratios $k_3; \text{Prim}(\text{OH}); \text{CHM}/k_3; \text{Sec}(\text{OH}); \text{CHD}$ (1.802, 1.875, 1.920, 1.977, 2.031) for $N_c = 2, 3, 4, 5, 6$, respectively) are smaller than the corresponding ones for the heterogeneous reactions of cellulose. These include acetylation (ratio = 4 ± 1) (Malm et al., 1953), acylation by palmitoyl chloride under reduced pressure (theoretically calculated ratio = 5); (Kwatra et al., 1992) tosylation by tosyl chloride in pyridine (ratio = 5.8) (Heuser, Heath, & Shockley, 1950), and etherification by the severely sterically crowded tris(p-tolyl)chloromethane (ratio = 4.3) (Jain, Agnish,

Table 2

Third order rate constants and activation parameters calculated for the imidazole-catalyzed acylation of microcrystalline cellulose, MCC in 4% LiCl/DMAC, at 70°C .^{a,b}

	Temperature				Anhydride		
	40°C	50°C	60°C	70°C	ΔH^\ddagger , kcal mol $^{-1}, c$	$T\Delta S^\ddagger$, kcal mol $^{-1}, c$	ΔG^\ddagger , kcal mol $^{-1}, c$
MCC; $10^3 \times (\text{overall } k_3)$, mol $^{-2} \text{ s}^{-1}$							
Ethanoic	3.395	4.560	5.934	7.510	4.97 (−0.8)	−18.53 (2.03)	23.50 (−2.83)
Propanoic	2.466	3.365	4.570	5.740	5.39 (−1.15)	−18.28 (1.57)	23.67 (−2.72)
Butanoic	1.865	2.530	3.540	4.620	5.84 (−1.21)	−17.98 (1.46)	23.82 (−2.67)
Pentanoic	3.105	4.125	5.290	6.465	4.55 (−1.54)	−19.04 (1.06)	23.59 (−2.60)
Hexanoic	3.650	4.645	5.710	6.870	3.81 (−2.21)	−19.74 (0.54)	23.55 (−2.75)
MCC; $10^3 \times k_3; \text{Prim}(\text{OH})$, mol $^{-2} \text{ s}^{-1}, d$							
Ethanoic	2.778	3.731	4.857	6.146	4.97 (−0.7)	−18.93 (1.98)	23.90 (−2.68)
Propanoic	2.032	2.773	3.766	4.731	5.39 (−1.06)	−18.68 (1.51)	24.07 (−2.57)
Butanoic	1.543	2.093	2.929	3.823	5.84 (−1.11)	−18.38 (1.33)	24.22 (−2.44)
Pentanoic	2.582	3.430	4.399	5.378	4.55 (−1.65)	−19.44 (0.89)	23.99 (−2.54)
Hexanoic	3.049	3.880	4.770	5.740	3.81 (−2.11)	−20.15 (0.36)	23.96 (−2.47)
MCC; $10^3 \times k_3; \text{Sec}(\text{OH})$, mol $^{-2} \text{ s}^{-1}, d$							
Ethanoic	0.308	0.414	0.538	0.682	4.97 (−0.71)	−20.45 (1.75)	25.42 (−2.46)
Propanoic	0.216	0.295	0.401	0.504	5.39 (−1.05)	−20.23 (1.31)	25.62 (−2.36)
Butanoic	0.160	0.218	0.305	0.398	5.84 (−1.11)	−19.94 (1.13)	25.78 (−2.24)
Pentanoic	0.261	0.347	0.445	0.543	4.55 (−1.78)	−21.03 (0.65)	25.58 (−2.43)
Hexanoic	0.300	0.382	0.469	0.565	3.81 (−2.11)	−21.76 (0.31)	25.57 (−2.42)

^a All rate constants and activation parameters were calculated/one hydroxyl group.

^b The activation parameters were calculated for the reaction at 70°C . The uncertainties in the activation parameters are $\pm 0.05 \text{ kcal mol}^{-1}$ (ΔH^\ddagger , and ΔG^\ddagger) and $0.2 \text{ cal K}^{-1} \text{ mol}^{-1}$ (ΔS^\ddagger).

^c The numbers within parenthesis refer to (activation parameter Imz-catalyzed reaction – uncatalyzed reaction).

^d The individual rate constants were calculated by splitting values of the overall k_3 by the following reactivity ratios: 9.010, 9.375, 9.600, 9.885, 10.155, for ethanoic-, propanoic-, butanoic-, pentanoic and hexanoic anhydride, respectively.

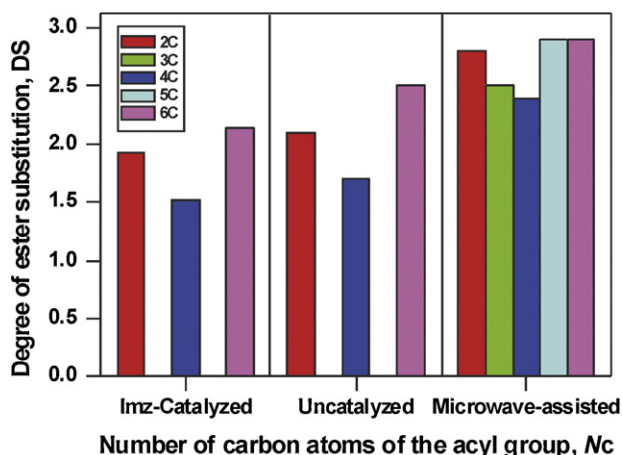


Fig. 3. Dependence of the degree of substitution of cellulose esters, DS, on the number of carbon atoms of the acyl group of RCOImz or $(\text{RCO})_2\text{O}$, N_c , whose value is shown in the insert. The results, from left to right refer to: Acylation by RCOImz in LiCl/DMAC (present work); uncatalyzed acylation by $(\text{RCO})_2\text{O}$, conventional heating in LiCl/DMAC (Nawaz et al., 2012); acylation by $(\text{RCO})_2\text{O}$, microwave heating in the ionic liquid in 3-allyl-1-methylimidazolium chloride (Possidonio, Fidale, & El Seoud, 2010).

Lal, & Bhatnagar, 1985). A possible reason for the smaller ratios is that the acylation of CHM and CHD has been carried out under homogenous conditions, where the hydroxyl groups are completely accessible. As discussed elsewhere; this is not the case for the OH groups of cellulose that is usually not present in molecular (i.e., non-aggregated) form (El Seoud & Heinze, 2005; Ramos, Morgado, El Seoud, da Silva, & Frollini, 2011). This difference in accessibility should result in larger

$k_{3;\text{Prim}(\text{OH}),\text{MCC}}/k_{3;\text{Sec}(\text{OH}),\text{MCC}}$, as compared with the corresponding ratios of the model compounds.

In order to address this point, we have calculated our data for MCC by multiplying $k_{3;\text{Prim}(\text{OH});\text{CHM}}/k_{3;\text{Sec}(\text{OH});\text{CHD}}$ by 5, the average value indicated above. These new ratios (9.010, 9.375, 9.600, 9.885, 10.155, for $N_c = 2, 3, 4, 5, 6$, respectively) were then employed in order to split the overall k_3 into contributions from the primary and secondary hydroxyl groups of MCC, resulting in the values reported in Table 1.

We have employed another approach in order to estimate the correction of $k_{3;\text{Prim}(\text{OH});\text{CHM}}/k_{3;\text{Sec}(\text{OH});\text{CHD}}$, based on the (theoretically calculated) volumes of the acylating agent, RCOImz: except for ethanoic anhydride- whose $k_{3;\text{Prim}(\text{OH});\text{CHM}}/k_{3;\text{Sec}(\text{OH});\text{CHD}}$ was maintained (1.802)- we multiplied each of the remaining rate constant ratios by the corresponding volume ratio ($V_{\text{RCOImz}}/V_{\text{CH}_3\text{COImz}}$), resulting the corrected values of (2.102, 2.390, 2.850, 3.048), for $N_c = 3, 4, 5, 6$, respectively; the results listed in Table SM-3. As expected, the values of ΔH^\ddagger are the same; the values of $T\Delta S^\ddagger$, hence of ΔG^\ddagger differ from those of Table 1 by ≤ 0.1 kcal/mol. That is, the procedure employed for splitting k_3 into its components bears little on the activation parameters, hence on the conclusions drawn.

(iv) The values within parenthesis in the last three columns of Table 1 show the reason for the observed catalysis. For all anhydrides studied, as compared with the uncatalyzed reaction, imidazole catalysis results in smaller enthalpy, and larger (i.e., less negative) entropy of activation. The reason of the smaller enthalpy may be traced to the above-mentioned higher electrophilic character of the acyl-carbon of RCOImz. The larger entropy of activation maybe attributed to the smaller volume of the acylating agent, RCOImz, as compared with the bulky

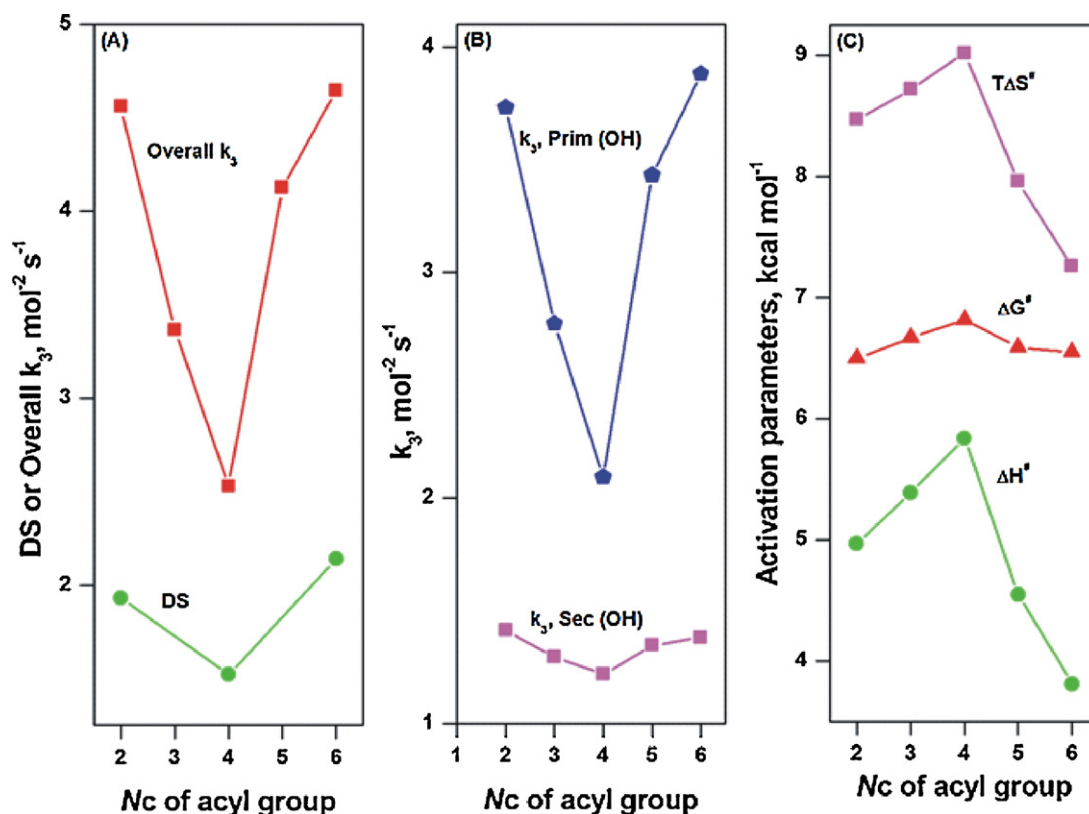


Fig. 4. Imz-catalyzed acylation of MCC; all plots are for the dependence on the number of carbon atoms of the acyl group of RCOImz, N_c : part (A); DS and k_3 ; part (B) $k_{3;\text{Prim}(\text{OH})}$ and $k_{3;\text{Sec}(\text{OH})}$; part (C) the activation parameters. For ease of visualization, the data have been plotted with the following modifications: part (A) ($10^3 \times k_3$); part (B) ($10^3 \times k_{3;\text{Prim}(\text{OH})}$), ($(10^3 \times k_{3;\text{Sec}(\text{OH})}) + 1$); part (C), ($T\Delta S^\ddagger + 27$) and ($\Delta G^\ddagger - 17$).

anhydride, see Eq. (3)

$$V_{R(\text{CO})\text{Imz}} = 1.142 + 0.324V_{R(\text{CO})2\text{O}} \quad r = 0.994 \quad \text{SD} = 0.0626 \quad (3)$$

- (v) An important objective of the present study is to determine the dependence of the results on N_c . Consider first the values of DS shown in Fig. 3. This contains data of the Imz-catalyzed reaction; and of the corresponding uncatalyzed acylation by carboxylic acid anhydrides, by using conventional- (i.e., by convection) or microwave heating. In all cases, the values of DS decrease on going from ethanoic- to butanoic-, then increase on going to hexanoic anhydride. Therefore, this behavior seems to be general, at least for acylation, independent of nature of acylating agent ($(\text{RCO})_2\text{O}$ or RCOImz), the method of heating; the solvent (electrolyte/dipolar aprotic or IL) (Koehler et al., 2007), or the type of cellulose (MCC or fibrous).

The reason for this dependence is shown in Fig. 4. Parts (A) and (B) show that there is a clear parallelism between the dependence on N_c of either DS, or the overall/individual rate constants. This is due to the enthalpy/entropy compensations that are clear in part (C). As an example, consider the results for k_3 . On going from ethanoic- to butanoic anhydride the (unfavorable) change in $|\Delta H^\ddagger|$ is 0.87 kcal/mol, whereas the (favorable) change in the $|T\Delta S^\ddagger|$ term is 0.55 kcal/mol. The corresponding changes on going from butanoic- to hexanoic anhydride are 2.03 and 1.76 kcal/mol for (favorable) $|\Delta H^\ddagger|$ and (unfavorable) $|T\Delta S^\ddagger|$, respectively. Therefore, the dependence of the rate constants, hence DS on N_c is complex due to subtle changes in the activation parameters, with the change in enthalpy dominating.

Although the variations in the activation parameters are admittedly small, they point out to a trend. The increase in ΔH^\ddagger on going from *N*-acetyl- to *N*-butanoylimidazole may be related to the decrease in the electrophilicity of the acyl group. The subsequent decrease in ΔH^\ddagger (*N*-butanoyl- to *N*-hexanoylimidazole) may be related to favorable hydrophobic interactions between the carbon chains of the *N*-acylimidazole and cellulosic surface, whose lipophilicity has increased, due to its partial acylation. The importance of hydrophobic interactions in cellulose chemistry has been recently advanced in order to explain some aspects of cellulose dissolution (Lindman, Karlström, & Stigsson, 2010; Medronho, Romano, Miguel, Stigsson, & Lindman, 2012), as well as its interactions with ionic liquids (Liu, Sale, Holmes, Simmons, & Singh, 2010). These cancellation effects lead to the subtle, but persistent variations of ΔG^\ddagger as a function of increasing N_c .

4. Conclusions

Esterification of cellulose by carboxylic acid anhydrides is efficiently catalyzed by imidazole. Spectroscopic data (^1H NMR; FTIR) and the results of theoretical calculations clearly show that the acylating agent is *N*-acylimidazole. The esterification reaction, however, is not subject to catalysis by TsCl . Conductivity is a convenient technique in order to study the kinetics of cellulose derivatization. The use of the model compounds CHM and CHD permits dividing the overall rate constants of cellulose catalyzed acylation into individual contributions from the primary and secondary hydroxyl groups of the AGU; the former is more reactive for all *N*-acylimidazoles; the selectivity for C6-OH increases as a function of increasing N_c . Unlike the biopolymer, the hydroxyl groups of the model compounds are readily accessible. More realistic ($k_{3,\text{Prim}(\text{OH}),\text{MCC}}/k_{3,\text{Sec}(\text{OH}),\text{MCC}}$) can be obtained, however, by simple corrections; the conclusions are practically independent of the correction approach employed. The kinetic results are satisfying because they show a parallelism between the effect of N_c on either the rate constants or the DS of

esters synthesized. The nonlinear dependence of DS on N_c appears to be general, independent of the nature of the acylating agent; the solvent employed; the type of cellulose, or the method of heating. In case of LiCl/DMAC , it is attributed to subtle, complex and compensating changes of the activation enthalpy and entropy.

5. Calculations

5.1. Theoretical calculations

5.1.1. Quantum mechanics calculations

For the calculation of the atomic charges, molar volumes and creation of the input for molecular dynamics, MD, simulations, all molecules have their geometries optimized (gas phase) by using DFT calculation, by employing B3LYP density functional and 6-311+g(d,p) basis set. To calculate the atomic charges, the (geometry optimized) ethanoic anhydride and *N*-acetylimidazole were solvated in DMAC by using the Polarizable Continuum Model (PCM) and their geometries were re-optimized. Mulliken population analysis was employed in order to calculate atomic charges. The numbering and optimized geometries are shown in Fig. SM-5; the atomic charges are shown in Table SM-3.

The molar volumes of the *N*-acylimidazoles after their geometries have been optimized in gas phase are shown in Table SM-4.

All calculations were done using Gaussian 09 rev. A.02 program package (Frisch et al., 2009).

5.1.2. Molecular dynamics simulations

Gromacs 4.0.7 software package has been employed for all MD simulations (Van Der et al., 2005). Two systems were simulated, each of them containing 250 DMAC molecules; 25 molecules of CHD, and either 100 molecules of ethanoic anhydride or *N*-acetylimidazole. The simulation was performed at 300 K, for 30 ns by using OPLS force field, isothermal-isobaric (NPT) ensemble, periodic boundaries and the smooth particle-mesh Ewald (PME) algorithm for long-range electrostatic interactions (Jorgensen, Maxwell, & Tirado-Rives, 1996). Equilibration of the ensemble was checked by monitoring the potential energy and density. The optimized geometry of CHD; ethanoic anhydride; and *N*-acetylimidazole were calculated as previously described in Section 5.1.1. OPLS-optimized DMAC geometry and topology was taken from literature (Caleman et al., 2012; Jorgensen & Tirado-Rives, 2005). The partial charges on the atoms were calculated by using the AM1 wave function via the CM1A approach (Storer, Giesen, Cramer, & Truhlar, 1995), as implemented in the AMSOL 7.1 program (Jorgensen, 1986; Kaminski & Jorgensen, 1998). A sub-routine implemented in the Gromacs program has been employed for calculating the number of molecules that remain in contact as a function of time (in ps). This refers to molecules that remain within 0.56 nm; the distance from (highly energetic) zero separation to the end of the first solvation shell, i.e., the end of the first peak in the radial distribution function between the (O) of CHD and the acyl carbonyl carbon of either $(\text{CH}_3\text{CO})_2\text{O}$, or $\text{N-CH}_3\text{COImz}$.

Acknowledgments

We thank TWAS (The Academy of Sciences for the Developing World) and CNPq (National Council for Scientific and Technological Research) for a pre-doctoral fellowship to H. Nawaz, and a productivity fellowship to O.A. El Seoud, and Fapesp (São Paulo research Foundation) for financial support. This work was carried out within the framework of INCT-Catálise.

Appendix A. Supplementary data

Supplementary data associated with this article can be found, in the online version, at <http://dx.doi.org/10.1016/j.carbpol.2012.10.009>.

References

- AIST Copyright©. (2001). *Spectral database for organic compounds SDBS*. http://riodb01.ibase.aist.go.jp/sdbs/cgi-bin/direct_frame_top.cgi [The SDBS No of the product CHM is 52821, accessed 23.07.11].
- Anslyn, E. V., & Dougherty, D. A. (2006). *Modern physical organic chemistry*. Sausalito: University Science Books., p. 382.
- Armagero, W. L. F., & Chai, C. L. L. (2003). *Purification of laboratory chemicals* (5th ed.). New York: Elsevier.
- ASTM D871-96. (2002). *Standard test methods of testing cellulose acetate* (solution method; procedure A).
- Buschle-diller, G., & Zeronian, S. H. (1992). Enhancing the reactivity and strength of cotton fibres. *Journal of Applied Polymer Science*, 45, 967–979.
- Caleman, C., van Maaren, P. J., Hong, M., Hub, J. S., Costa, L. T., & van der Spoel, D. (2012). Force field benchmark of organic liquids: Density, enthalpy of vaporization, heat capacities, surface tension, isothermal compressibility, volumetric expansion coefficient, and dielectric constant. *Journal of Chemical Theory and Computation*, 8, 61–74.
- Das, B., Reddy, V. S., & Tehseen, F. (2006). A mild, rapid and highly regioselective ring-opening of epoxides and aziridines with acetic anhydride under solvent-free conditions using ammonium-12-molybdophosphate. *Tetrahedron Letters*, 47, 6865–6868.
- El Seoud, O. A., Menegheli, P., Pires, P. A. R., & Kiyan, N. (1994). Kinetics and mechanism of the imidazole-catalyzed hydrolysis of substituted N-benzoylimidazoles. *Journal of Physical Organic Chemistry*, 7, 431–436.
- El Seoud, O. A., & Heinze, T. (2005). Organic esters of cellulose: New perspectives for old polymers. *Advance Polymer Science*, 186, 103–149.
- Frisch, M. J., Trucks, G. W., Schlegel, H. B., Scuseria, G. E., Robb, M. A., Cheeseman, J. R., et al. (2009). *Gaussian 09. Revision A.02*. Wallingford, CT: Gaussian, Inc.
- Hacon, J., Morris, A., Johnston, M. J., Shanahan, S. E., Barker, M. D., Inglis, G. G. A., et al. (2007). Carbon–carbon bond forming reactions with substrates absorbed non-covalently on a cellulose chromatography paper support. *Chemical Communications*, 6, 625–627.
- Heuser, E., Heath, M., & Shockley, Wm. H. (1950). The rate of esterification of primary and secondary hydroxyls of cellulose with p-toluenesulfonyl (tosyl) chloride. *Journal of the American Chemical Society*, 72, 670–674.
- Hussain, A. M., Liebert, T., & Heinze, T. (2004). Acylation of cellulose with N,N-carboxyldiimidazole-activated acids in the novel solvent dimethyl sulfoxide/tetrabutylammonium fluoride. *Macromolecular Rapid Communications*, 25, 916–920.
- Jain, R. K., Agnish, S. L., Lal, K., & Bhatnagar, H. L. (1985). Reactivity of hydroxyl groups in cellulose towards chloro(p-tolyl)methane. *Macromolecular Chemistry and Physics*, 186, 2501–2512.
- Jorgensen, W. L. (1986). Optimized intermolecular potential functions for liquid alcohols. *Journal of Physical Chemistry*, 90, 1276–1284.
- Jorgensen, W. L., Maxwell, D. S., & Tirado-Rives, J. (1996). Development and testing of the OPLS all-atom force field on conformational energetics and properties of organic liquids. *Journal of the American Chemical Society*, 118, 11225–11236.
- Jorgensen, W. L., & Tirado-Rives, J. (2005). Chemical theory and computation special feature: potential energy functions for atomic-level simulations of water and organic and biomolecular systems. *Proceedings of the National Academy of Sciences of the United States of America*, 102, 6665.
- Kaminski, G. A., & Jorgensen, W. L. (1998). A quantum mechanical and molecular mechanical method based on CM1A charges: Applications to solvent effects on organic equilibria and reactions. *Journal of Physical Chemistry B*, 102, 1787–1796.
- Kenichi, T. (2003a). *Preparation of sulfonic acid anhydrides*. Jpn. Kokai Tokkyo Koho (JP 2003277345 A 20031002).
- Kenichi, T. (2003b). *Purification of sulfonic acid anhydrides*. Jpn. Kokai Tokkyo Koho (JP 2003238522 A 20030827).
- Khaja, S. D., & Xue, J. (2006). Ceric ammonium nitrate: Novel and robust acetylating catalyst. *Letters in Organic Chemistry*, 3, 554–557.
- Koehler, S., Liebert, T., Schoebitz, M., Schaller, J., Meister, F., Guenther, W., et al. (2007). Interactions of ionic liquids with polysaccharides 1. Unexpected acetylation of cellulose with 1-ethyl-3-methylimidazolium acetate. *Macromolecular Rapid Communications*, 28, 2311–2317.
- Kondo, T. (1993). Preparation of 6-O-alkylcelluloses. *Carbohydrate Research*, 238, 231–240.
- Kwatra, H. S., Caruthers, J. M., & Tao, B. Y. (1992). Synthesis of long chain fatty acids esterified onto cellulose via the vacuum-acid chloride process. *Industrial & Engineering Chemistry Research*, 31, 2647–2651.
- Lide, D. R. (2004). In D. R. Lide (Ed.), *CRC handbook of chemistry and physics*. Boca Raton, FL: CRC Press.
- Lindman, B., Karlström, G., & Stigsson, L. (2010). On the mechanism of dissolution of cellulose. *Journal of Molecular Liquids*, 156, 76–81.
- Liu, H., Sale, K. L., Holmes, B. M., Simmons, B. A., & Singh, S. (2010). Understanding the interactions of cellulose with ionic liquids: A molecular dynamics study. *Journal of Physical Chemistry B*, 114, 4293–4301.
- Liu, Y., Liu, L., Lu, Y., & Cai, Y.-Q. (2008). An imidazolium tosylate salt as efficient and recyclable catalyst for acetylation in an ionic liquid. *Monatshefte fuer Chemie*, 139, 633–638.
- Malm, C. J., Tanghe, L. O., Laird, B. C., & Smith, G. D. (1953). Relative rates of acetylation of the hydroxyl groups in cellulose acetate. *Journal of the American Chemical Society*, 75, 80–84.
- Medronho, B., Romano, A., Miguel, M.-G., Stigsson, L., & Lindman, B. (2012). Rationalizing cellulose (in) solubility: Reviewing basic physicochemical aspects and role of hydrophobic interactions. *Cellulose*, 19, 581–587.
- Menger, F. M. (1985). On the source of intramolecular and enzymatic reactivity. *Accounts of Chemical Research*, 18, 128–134.
- Nawaz, H., Casarano, R., & El Seoud, O. A. (2012). First report on the kinetics of the uncatalyzed esterification of cellulose under homogeneous reaction conditions: A rationale for the effect of carboxylic acid anhydride chain-length on the degree of biopolymer substitution. *Cellulose*, 19, 199–207.
- Possidonio, S., Fidale, L. C., & El Seoud, O. A. (2010). Microwave -assisted derivatization of cellulose in an ionic liquid: An efficient, expedient synthesis of simple and mixed carboxylic esters. *Journal of Polymer Science, Part A: Polymer Chemistry*, 48, 134–143.
- Press, W. H., Teukolsky, S. A., Vetterling, W. T., & Flannery, B. P. (2007). *Numerical recipes: The art of scientific computing* (3rd edn). Cambridge: Cambridge University Press.
- Ramos, L. A., Assaf, J. M., El Seoud, O. A., & Frollini, E. (2005). Influence of the supramolecular structure and physicochemical properties of cellulose on its dissolution in a lithium chloride/N,N-dimethylacetamide solvent system. *Biomacromolecules*, 6, 2638–2647.
- Ramos, L. A., Morgado, D. L., El Seoud, O. A., da Silva, V. C., & Frollini, E. (2011). Acetylation of cellulose in LiCl-N,N-dimethylacetamide: First report on the correlation between the reaction efficiency and the aggregation number of dissolved cellulose. *Cellulose*, 18, 385–392.
- Storer, J. W., Giesen, D. J., Cramer, C. J., & Truhlar, D. G. (1995). Class IV charge models: A new semiempirical approach in quantum chemistry. *Journal of Computer-Aided Molecular Design*, 9, 87–110.
- Tosh, B., & Saikia, C. N. (2000). Preparation of cellulose pentanoate of different degree of substitution: A detailed kinetics study. *Trends in Carbohydrate Chemistry*, 6, 143–153.
- Tosh, B., Saikia, C. N., & Dass, N. N. (2000). Homogeneous esterification of cellulose in the lithium chloride- N,N-dimethylacetamide solvent system: Effect of temperature and catalyst. *Carbohydrate Research*, 327, 345–352.
- Van Der Spoel, D., Lindahl, E., Hess, B., Groenhof, G., Mark, A. E., et al. (2005). GROMACS: Fast, flexible, and free. *Journal of Computational Chemistry*, 26, 1701–1718.
- Zeynizadeh, B., & Sadighnia, L. (2010). A green protocol for catalytic conversion of epoxides to 1,2-diacetoxy esters with phosphomolybdic acid alone or its supported on silica gel. *Bulletin of the Korean Chemical Society*, 31, 2644–2648.
- Zeynizadeh, B., & Sadighnia, L. (2011). One-pot catalytic conversion of epoxides to 1,2-diacetates with hydride transferring agents in acetic anhydride. *Synthetic Communications*, 41, 637–644.